Journal of Thermal Analysis and Calorimetry, Vol. 94 (2008) 3, 649–653

SYNTHESIS OF MESOPOROUS SILICAS INSIDE LARGE PORES OF INORGANIC MATRIX

I. S. Berezovska[*]*, V. V. Yanishpolskii and V. A. Tertykh*

O. O. Chuiko Institute of Surface Chemistry of National Academy of Sciences of Ukraine, General Naumov Str. 17 03164 Kyiv, Ukraine

Template syntheses of mesoporous silicas have been carried out inside large pores of inorganic matrix. Portions of tetraethoxysilane and cetyltrimethylammonium bromide micellar solution were incorporated step-by-step inside pore volume of silica gel with large pore size. Synthesized materials were characterized using thermal analysis, adsorption-desorption of nitrogen and X-ray diffraction scattering.

Keywords: *large pores, mesoporous silica, silica gel, template synthesis*

Introduction

Template synthesis of mesoporous ordered silica matrices is considered to be one of the most important trends in nanostructural materials science. Together with successes in porous structure design, an increase of ordered mesoporous silicas stability is a crucial parameter in their potential application. M41S collapse when they are mechanically compressed and have a poor hydrothermal stability in boiling water due to silicate hydrolysis of the relative thin amorphous silica walls [1–3]. Because of these limitations exceeding efforts have been made to improve the stability of M41S materials by either changing the synthesis procedure or by postsynthetic modification. Generally, structural and hydrothermal stability of nanoporous silica materials can be improved by increasing the wall thickness and enhancing the local ordering of the amorphous walls [4] or by hydrophobization of silica surface [5]. Other reports have illustrated that MCM-41 and MCM-48 with metals incorporated into framework have higher mechanical and hydrothermal stability [1, 6–10]. Recently several other strategies have been successfully developed for synthesis of HMS and SBA type mesostructures with consistently larger framework wall thicknesses than those of MCM-41 and MCM-48 [11, 12]. However, no remarkable trends could be observed for the mechanical stability of M41S and the mesoporosity is essentially lost for all mesostructures at pressure of approximately 444 MPa. All ordered mesoporous structures show an inferior mechanical stability compared with zeolites. This may result from their large porosity and the absence of stabilizing crystal structure. Therefore to upgrade the performance of mesoporous molecular sieves and zeolites, much effort has been undertaken to synthesize new types of materials, which would combine the advantages of these two kinds of molecular sieves [13–17]. Finally it should be mentioned that, despite the very interesting features of the mesostructures assembled from zeolite seeds, much work has still to be done to enhance mechanical stability of mesoporous silicas. In the present paper, improvement of mechanical properties by incorporation of MCM-41 materials inside pore volume of silicas with higher structural stability has been proposed.

Experimental

Syntheses of mesoporous silicas were carried out according to procedure [18] with a use of tetraethoxysilane (TEOS) and cetyltrimethylammonium bromide (CTAB). Formed micellar solutions were introduced inside pores volume of silica gel with specific surface area of 115 $m^2\ g^{-1}$ and pore size of about 24 nm. The main condition for successful template synthesis inside silica gel matrices was high value of TEOS/H_2O molar ratio. Molar ratio of solution components was 1TEOS:0.18CTAB:5NH_3:75H_2O. Introduction of micellar solution inside pore volume of silica gel was realized step-by-step according to six procedures.

Procedure I (the first introduction of TEOS and CTAB micellar solution inside silica gel pore volume)

CTAB (3 g, 0.008 mol) was dissolved in water (50 mL, 2.8 mol). Solution was stirred for 10 min and

* Author for correspondence: berinna2003@rambler.ru

1388–6150/$20.00

Akadémiai Kiadó, Budapest, Hungary
Springer, Dordrecht, The Netherlands

then TEOS (10 cm^3, 0.045 mol) was added. Gel was mixed for 5 min and then 12 g of silica gel was added. In an hour the sample was filtered and 25% ammonia (15 cm^3, 0.2 mol) was introduced. After 12 h synthesized composite was filtered and washed with water by decantation to remove MCM-41 out of silica gel external surface. Then the samples were dried for 2 h at 363 K to evaporate residual water and ammonia. A weighed portion of composite (2 g) was calcined for 5 h at 823 K and used for structure-adsorption characteristics measurements. Residual portion (10 g) was used for the second introduction of micellar solution.

Procedure II (the second introduction of TEOS and CTAB micellar solution inside silica gel pore volume)

A weighed portion of CTAB (2.5 g, 0.0067 mol) was dissolved in water (42 cm^3). After stirring for 10 min, TEOS (8.3 cm^3, 0.036 mol) was added. Gel was mixed for 5 min and then 10 g of sample synthesized in procedure I was added. The solution was kept for an hour, after filtration of precipitate, 25% ammonia (12.5 cm^3, 0.165 mol) was added. In 12 h silica was filtered and decanted with water until the solution became clear. Synthesized material was dried at 363 K for 2 h. 2 g of synthesized sample was calcined for 5 h at 823 K to remove organic template and 8 g of uncalcined composite was used for further MCM-41 introduction.

Procedure III (the third introduction of TEOS and CTAB micellar solution inside silica gel pore volume)

CTAB (2 g, 0.0053 mol) was dissolved in water (33 cm^3, 1.86 mol) and stirred for 10 min. After introduction TEOS (6.7 cm^3, 0.03 mol) and stirring for 5 min, the sample synthesized in the second procedure (8 g) was added. In an hour the solution was filtered and the precipitate was immersed into ammonia solution (10 cm^3, 0.14 mol). The sample was kept for 12 h and dried for 2 h at 90°C following the filtration and decantation. The weighed portion of composite (6 g) was left for the next procedure; another portion (2 g) was calcined at 823 K.

Procedure IV (the fourth introduction of TEOS and CTAB micellar solution inside silica gel pore volume)

CTAB (1.5 g, 0.0039 mol) was dissolved in a flask with water (25 cm^3, 1.5 mol) and stirring for 10 min. TEOS (5 cm^3, 0.0225 mol) was introduced into formed micellar solution. After stirring for 5 min the silica gel synthesized in the previous procedure was added. In an hour the formed precipitate was filtered, followed by washing with 25% ammonia solution (7.5 cm^3, 0.1 mol) and dried for 2 h at 363 K. One part of synthesized composite (4 g) was used for the next procedure; another (2 g) was calcined for 5 h at 823 K.

Procedure V (the fifth introduction of TEOS and CTAB micellar solution inside silica gel pore volume)

Solution of CTAB (1 g, 0.0028 mol) and water (16.6 cm^3, 0.93 mol) was mixed for 10 min and TEOS (2.35 cm^3, 0.015 mol) was introduced. After stirring for 5 min silica gel synthesized in the fourth procedure was added. The sample was kept for an hour in micellar solution, then filtered and 25% ammonia solution (5 cm^3, 0.066 mol) was introduced; after 12 h the composite was filtered, decanted and dried for 2 h at 363 K. Synthesized composite was divided in half. One part was calcined for 5 h at 823 K to remove organic template. Another one was used for complete micellar solution infill of pore volume.

Procedure VI (the sixth introduction of TEOS and CTAB micellar solution inside silica gel pore volume)

CTAB (0.5 g, 0.0013 mol) was dissolved in water (8.3 cm^3, 0.467 mol) and mixed for 10 min, and then TEOS (1.7 cm^3, 0.0075 mol) was introduced and mixed for 5 min with a magnetic stirrer. Silica gel synthesized in previous procedure (2 g) was immersed into formed solution and in an hour the precipitate was filtered and ammonia solution (2.5 cm^3, 0.033 mol) was added. In 12 h synthesized composite was filtered, washed and dried for 2 h at 363 K. Synthesized sample was studied by thermogravimetric analysis (TG) using derivatograph Q-1500 Paulik–Paulik–Erdey (Hungary), the heating rate was 10°C min^{-1}.

The calcined silicas synthesized according to above-described procedures were investigated by adsorption-desorption of nitrogen at 77 K (ASAP-2000). From isotherms of nitrogen adsorption the specific surface area and pore volume were calculated by BET equation, and pore size distribution was determined by BJH-method. The structure of samples was studied using small-angle X-ray diffraction (XRD) (automated diffractometer DRON-4-07, CuK_α-radiation).

Results and discussion

Results of thermal analysis of template-containing mesoporous silicas synthesized inside pore volume of silica gel are presented in Fig. 1.

TG studies of uncalcined samples can provide the information about the interaction of the associated

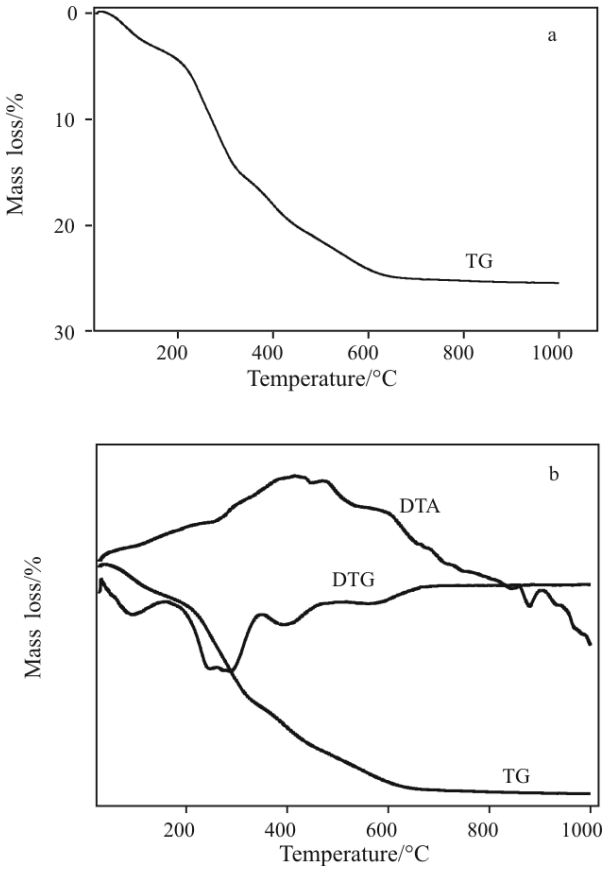

Fig. 1 a – TG, b – DTG and DTA curves of mesoporous silicas synthesized inside pores volume of silica gel

template with surface silanol groups and approximate content of organic template. As can be seen from Fig. 1, TG and DTG curves of synthesized materials show a typical decomposition profile with four distinctive mass loss steps. Initial mass loss (about 4%) at the temperature up to 200°C can be explained by evaporation of ammonia and physically adsorbed water. In the temperature range from 200 up to 360°C the main decrease of mass (about 12%) with expressed exothermal effect (DTA curve) is observed because of organic template decomposition. The third peak on DTG curve in the temperature range 360–550°C is connected with thermal oxidation of residual organic compounds (about 7% mass loss). At the temperature above 550°C TG and DTG curves show slight mass loss (2.9%) corresponding to water loss due to condensation of silanol groups to form siloxane bonds. Total mass loss was 25.9 and 19% mass loss correspond to content of organic template. According to molar ratio of micellar solution the quantity of synthesized mesoporous silicas should be equal to 20% of total sample mass; this is in a good agreement with results of thermal analysis.

Nitrogen adsorption-desorption isotherm for silica gel is type III in the IUPAC classification [19]. The hysteresis loop of desorption branch at high relative pressure reveals the existence of large pores in the samples. Nitrogen adsorption-desorption isotherms of silica gel after template syntheses inside nanopores are characterized by the ranges capillary condensation ($0.3<p/p_o<0.4$) being evidence of the uniform mesopores presence. The sharpness of capillary condensation regions was increased after each template synthesis and was accompanied with

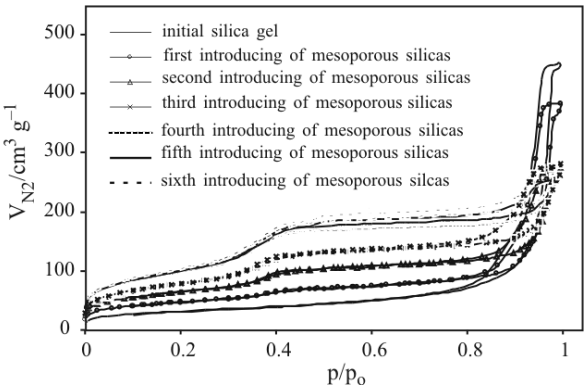

Fig. 2 Nitrogen adsorption-desorption isotherms for initial silica gel and silica matrices after template syntheses inside nanopores

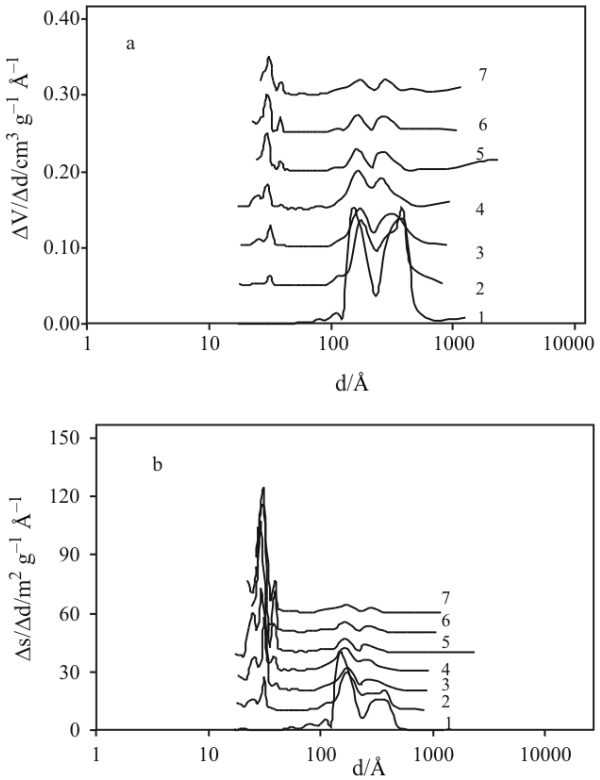

Fig. 3 Differential curves of dependence of pore size on a – pore volume and b – surface area for silicas incorporated inside large pores of silica gel: 1 – initial silica gel and 2 – silica gels after the first, 3 – the second, 4 – the third, 5 – the fourth, 6 – the fifth, 7 – the sixth introduction of MCM-41

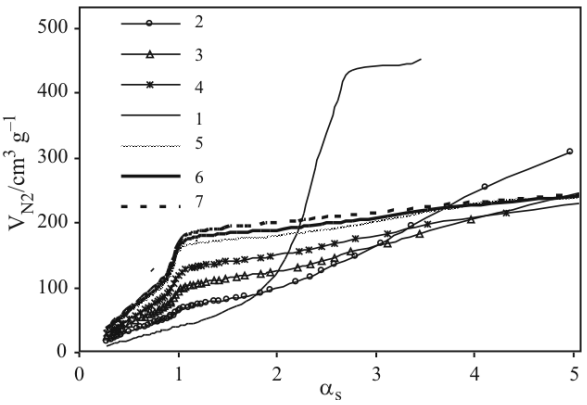

Fig. 4 α_s-plots of nitrogen at 77 K for initial silica gel and silica matrices after template syntheses inside nanopores (numbers correspond to samples in Table 1)

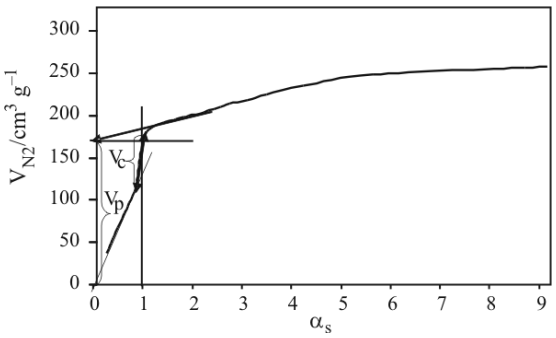

Fig. 5 α_s-plot of nitrogen at 77 K for silica after the sixth introduction of micellar solution, V_p – pore volume, V_c– core volume

decreasing of hysteresis loop that can be explained by filling of silica gel pore volume with mesoporous silicas. Specific surface areas of silica gel was 115 m^2 g^{-1} (by the BET equation) and the BJH pore size distribution curve for silica gel has a broad peak in the range of pore size 30–50 nm (Fig. 3, curve 1). Samples with incorporated mesoporous silicas are characterized by increase in specific surface area from 115 to 377 m^2 g^{-1} (Fig. 2). Pore size distribution curves exhibit the presence of peaks corresponding to pores of 2.5 nm size (Fig. 3).

One of the promising approaches to adsorption data analysis is based on the comparison of synthesized porous materials with the adsorption isotherms of the reference solid. Standard α_s-plots for synthesized silicas (Fig. 4) are suitable for evaluation of specific surface area, external surface area, micropore volume and primary mesopore volume of various adsorbents [19–21].

Sing *et al.* proposed the α_s-method to estimate the surface area of the test adsorbent

$$S_{\alpha s} = (V_{\text{test. }(\alpha s=1)}/V_{\text{std. }(\alpha s=1)})\cdot S_{\text{BET(std.)}}$$

Table 1 Structural-adsorption characteristics of synthesized silicas

No.	Procedure	S_{BET}/m^2 g^{-1}	α_s-analysis					
			S_t/m^2 g^{-1}	S_{ex}/m^2 g^{-1}	S_p/m^2 g^{-1}	V_p/cm^3 g^{-1}	V_c/cm^3 g^{-1}	r_p/nm
1	Initial silica gel	115	116	–	–	0.62	–	–
2	1st introduction of micellar solution	170	173	–	–	0.54	0.02	1.5
3	2nd introduction of micellar solution	233	237	–	–	0.34	0.03	1.3
4	3rd introduction of micellar solution	283	289	11.56	277	0.32	0.06	1.3
5	4th introduction of micellar solution	349	347	5.78	341	0.34	0.08	1.3
6	5th introduction of micellar solution	362	364	5.78	358	0.35	0.10	1.4
7	6th introduction of micellar solution	377	376	5.78	370	0.36	0.11	1.4

where $S_{BET(std.)}$ and $V_{std.}$ are surface area ($m^2\ g^{-1}$) and adsorbed amount ($cm^3\ g^{-1}$) at p/p_o=0.4 for the standard nonporous silica, respectively; $V_{test(\alpha s=1)}$ is the absorbed amount ($cm^3\ g^{-1}$) at p/p_o=0.4 for the test adsorbent [19]. The results obtained from analysis of the α_s-plots are summarized in Table 1 together with the BET surface area (S_{BET}).

Detailed analysis of α_s-plot for the sample 6 is presented in Fig. 5. From α_s-data the surface areas of synthesized materials were estimated using the Sing equation. The slope of the steep line gives the total surface area $S_t(N_2)$, while the slope of the less steep line provides the external surface area $S_{ex}(N_2)$. The pore area $S_p(N_2)$ is estimated from the difference between $S_t(N_2)$ and $S_{ex}(N_2)$. As seen from Table 1, S_{BET} is in good agreement with $S_t(N_2)$.

It has been proposed in previous investigations that the pores of MCM-41 adsorbents are assumed to be cylindrical and uniform [22]. For the cylindrical pore, the following relation is used to determine pore radius:

$$r_p(N_2) = 2V_p(N_2)/S_p(N_2)$$

Absence of any peaks at the diffractogram of initial silica gel confirms its amorphous nature (Fig. 6. curve 1). It is clear from X-ray diffraction patterns that introduction of micellar solution causes the appearance of reflections in low-angle region (Fig. 4. curves 2–7). Broad low angle diffraction peak should be the result of the formation of wormlike pore structure and weak intensity of reflection can be explained by small quantity of incorporated silicas (3% of the sample total mass after the sixth introduction of micellar solution).

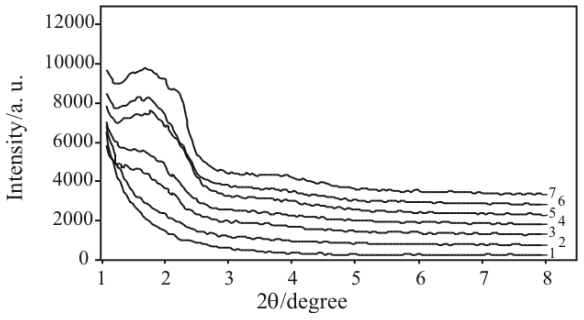

Fig. 6 X-ray diffractograms of silicas incorporated inside large pores of silica gel: 1 – initial silica gel and 2 – silica gels after the first, 3 – the second, 4 – the third, 5 – the fourth, 6 – the fifth, 7 – the sixth introduction of MCM-41

Conclusions

Present synthetic procedures are good combinations of template synthesis and conventional sol–gel process and they were executed in two stages. At the first stage silica gel was impregnated with micellar solution and at the second stage ammonia was added to catalyze hydrolysis and condensation of TEOS to provide mesoporous silicas formation. Template synthesis of mesoporous silicas with pore diameter of 2.5 nm was carried out inside nanoreactors based on large pores of silica gel. Surface area of initial silica gel was 115 $m^2\ g^{-1}$ and after step-by-step introduction of micellar solution calcined samples had surface area about 377 $m^2\ g^{-1}$.

References

1 P. Van Der Voort, M. Baltes and E. F. Vansant, Catal. Today, 68 (2001) 121.
2 S. Kawi and S.-C. Shen, Mater. Lett., 42 (2000) 108.
3 S. Jun, J. M. Kim, R. Ryoo, Y.-S. Ahn and M.-K. Han, Micropor. Mesopor. Mater., 41 (2000) 119.
4 R. Mokaya, J. Phys. Chem., B 103 (1999) 10204.
5 J. Goworek, W. Stefaniak, A. Kierys and M. Iwan, J. Therm. Anal. Cal., 87 (2007) 217.
6 A. Braileanu, M. Raileanu, M. Crisan, D. Crisan, R. Birjega, V. E. Marinescu, J. Madarász and G. Pokol, J. Therm. Anal. Cal., 88 (2007) 163.
7 R. Mokaya and W. Jones, Chem. Commun., (1998) 1839.
8 S.-C. Shen and S. Kawi, J. Phys. Chem., B 103 (1999) 8870.
9 S. D'arbonneau, A. Tuel and A. Auroux, J. Therm. Anal. Cal., 56 (1999) 287.
10 E. Molnár, Z. Konya and I. Kiricsi, J. Therm. Anal. Cal., 79 (2005) 573.
11 P. T. Tanev and T. J. Pinnavaia, Chem. Mater., 8 (1996) 2068.
12 M. Kruk, M. Jaroniec, C. H. Ko and R. Ryoo, Chem. Mater., 12 (2000) 1961.
13 P. E. A. De Moor, T. P. M. Beelen and A. van Santen, J. Phys. Chem., B 103 (1999) 36.
14 A. Firouzi, F. Atef, A. G. Oertli, G. D. Stucky and D. F. Chmelka, J. Am. Chem. Soc., 119 (1997) 3596.
15 Y. Liu, W. Zhang and T. J. Pinnavaia, J. Am. Chem. Soc., 122 (2000) 8791.
16 Z. Zhang, Y. Han and F.-S. Xiao, J. Am. Chem. Soc., 123 (2001) 5014.
17 D. T. On and S. Kaliaguine, Angew. Chem. Int. Sd., 41 (2002) 1036.
18 X. Wang, W. Li, G. Zhu, S. Qiu, D. Zhao and B. Zhong, Micropor. Mesopor. Mater., 71 (2004) 87.
19 S. J. Gregg and K. S. W. Sing, Academic Press, London 1967, p. 303.
20 M. Hakuman and H. Naono, J. Colloid Interface Sci., 241 (2001) 127.
21 M. Jaroniec and M. Kruk, Langmuir, 15 (1999) 5410.
22 C. T. Kresge, M. E. Leonowicz, W. J. Roth, J. C. Vartuli and J. S. Beck, Nature, 359 (1992) 710.

DOI: 10.1007/s10973-008-9361-z